processes

MDPI

Article

Comprehensive Evaluation Index System and Application of Low-Carbon Resilience of Power Grid Containing Phase-Shifting Transformer under Ice Disaster

Jing Zhang [1], Huilin Cheng [2], Peng Yang [3], Bingyan Zhang [4], Shiqi Zhang [4] and Zhigang Lu [4,*]

[1] Jinzhou County Power Supply Company, State Grid Hebei Electric Power Co., Ltd., Jinzhou 052200, China; liuyujie@stumail.ysu.edu.cn
[2] Shijiazhuang Power Supply Company, State Grid Hebei Electric Power Co., Ltd., Shijiazhuang 050051, China; chenghuilin2006@126.com
[3] State Grid Hebei Electric Power Co., Ltd., Shijiazhuang 050051, China; cindela_yp@163.com
[4] Key Laboratory of Power Electronics for Energy Conservation and Motor Drive of Hebei Province, Yanshan University, Qinhuangdao 066004, China; zhangbingyan01@126.com (B.Z.); shiqiz@stumail.ysu.edu.cn (S.Z.)
* Correspondence: zhglu@ysu.edu.cn

Abstract: In view of the high impact of extreme disasters, this paper comprehensively evaluates power grid performance from a new low-carbon toughness perspective. First, considering the increase in carbon emissions and the recovery time of carbon emissions, low-carbon resilience indicators are proposed. At the same time, considering the power-regulation effect of the phase-shifter transformer, the fault and response model of a power grid under an ice disaster is established, and then, a comprehensive evaluation index system of low-carbon toughness of the power grid is constructed. The weight determination is carried out using the fuzzy analytic hierarchy process-entropy-based weight method, while the fuzzy comprehensive evaluation center of gravity method is used to evaluate the power grid comprehensively. Finally, examples are presented to verify the feasibility of the proposed method, emphasizing its potential for evaluating the comprehensive performance of low-carbon and toughness of the power grid in the future.

Keywords: ice disaster; phase-shifting transformer; low-carbon resilience indicators; fuzzy comprehensive evaluation

Citation: Zhang, J.; Cheng, H.; Yang, P.; Zhang, B.; Zhang, S.; Lu, Z. Comprehensive Evaluation Index System and Application of Low-Carbon Resilience of Power Grid Containing Phase-Shifting Transformer under Ice Disaster. *Processes* **2023**, *11*, 2633. https://doi.org/10.3390/pr11092633

Academic Editors: Hongyu Wu and Bo Liu

Received: 6 July 2023
Revised: 10 August 2023
Accepted: 19 August 2023
Published: 4 September 2023

1. Introduction

Natural disasters, such as typhoons, torrential rains, and ice storms, have become increasingly frequent in recent years, significantly impacting the safe and steady operation of power grids. Transmission networks, including overhead transmission lines and towers, are susceptible to extreme weather events due to their prolonged exposure to the elements. The resulting faults can trigger widespread power outages and cascading reactions, even leading to grid collapse. The power system's research community has conducted extensive studies on grid resilience, focusing on resistance, adaptation, and recovery processes following disruptions typically through dynamic assessments of extreme events [1]. Under the new background of energy transition, Ref. [2] proposes that generalized resilient grids should have six key characteristics in addition to the three core characteristics of grid strain, defense, and resilience, while also paying attention to perception, collaboration, and learning. An optimal decision support system (DSS) for the operation of microgrids in extreme weather is proposed in [3] to maximize system autonomy. At present, relevant research on grid resilience assessment and improvement is also gradually being carried out. Ref. [4] presents a strategy for providing high system resilience at minimal cost under the influence of extreme weather events. Considering the two stages of disaster prevention and mitigation, an index system, including the defense time of the distribution

network, elastic recovery coefficient, island sustainable time, and mean outage time of important load, is constructed in Ref. [5]. Ref. [6] establishes a framework for evaluating the resilience of distribution systems under disasters and proposes a new quantitative evaluation index for resilience by analyzing the impact of various potential hazards on distribution network lines. In [7], an optimal power system partition recovery model that considers grid reconfiguration efficiency and path reliability is proposed to enhance the resilience of post-disaster systems. However, most of the existing literature studying resilience indicators and improvement measures for power grids neglect the effect of carbon emissions during disasters. The first paper to integrate resilience with low-carbon power grids is [8], which proposes three new characteristics: affordability for preventive measures, accessibility for post-disaster recovery, and sustainability for long-term planning. The article also highlights the risks posed by integrating high proportions of renewable energy into the grid, including the randomness and intermittency of wind and solar power, which can compromise safety and stability [9]. The widespread use of wind and solar power can reduce the system's inertia and security margin since they do not provide rotational inertia [10]. The combined risks of external threats, increased internal and external risk sources, and the uncertainty associated with low-carbon technologies have exacerbated safety issues in power grids [8]. Hence, while striving to achieve the dual-carbon goal, resilience issues resulting from new energy access must not be overlooked.

When a power system fails, the power distribution of the system often cannot guarantee power supply safety. To address this issue, the power flow control method using phase-shifting transformers is typically adopted to adjust line transmission power. This method can effectively and flexibly control the power flow without altering the original generating power and network topology. By applying a suitable voltage vector to the input voltage on the original line, the voltage phase difference changes on both sides of the line [11], improving power flow distribution and reducing line loss during system failure. Ref. [12] investigates the role of phase-shifting transformers in achieving forced power flow distribution under line overload conditions. Ref. [13] establishes a unified formula for the parameter correction equation of the phase-shifting transformer, enabling the control of active and reactive power flow in the system. Therefore, this paper aims to enhance the power grid's performance by including phase-shifting transformers in the transmission lines based on the conventional model.

To sum up, the existing research mostly considers the resilience of systems under extreme disasters and does not take into account the impact of changes in carbon emissions. To solve this problem, this paper constructs a comprehensive evaluation index system of low-carbon resilience of power grids under extreme disasters to evaluate the overall performance of the power grid.

The main contributions are as follows:

(1) According to the concept of low-carbon resilience (LCR), the evaluation index of low-carbon toughness is put forward. Compared with the traditional single resilience evaluation index, the LCR level of power grids under extreme disasters is measured from two new angles of carbon emission change and carbon emission recovery time.
(2) Considering the equivalent model of the branch with the phase-shifter transformer, the power flow distribution of the line is adjusted through the power regulation of the phase-shifter transformer so as to improve the transmission capacity of the power grid.
(3) Considering the impact of the whole process of disaster occurrence on the power grid, we build a comprehensive assessment index system for low-carbon resilience of the power grid; the principal comprehensive weight determination method combined with the fuzzy analytic hierarchy method (FAHP) and anti-entropy weight method (AEWM) is used, and the fuzzy evaluation value obtained is accurately processed with the center of gravity method (COG).

The other parts of this article are arranged as follows: Section 2 introduces the concept of LCR and LCR Power Network, Section 3 constructs the comprehensive evaluation index

system, Section 4 introduces the evaluation index method, Section 5 discusses the case study, and Section 6 puts forward the main conclusions.

2. LCR

2.1. LCR Concept

Low-carbon resilience (LCR) is based on the concept of resilience theory, which aims to improve the power grid's ability to cope with the increasing carbon emissions resulting from human activities. The goal of LCR is to accelerate emission reduction and enable mutual adaptation between social development and carbon emissions [14]. LCR is defined as the ability to maintain low levels of carbon emissions in human life and production while also emphasizing mitigation, emission reduction, and adaptation under the sustainable development goals. The continuous improvement of resilient power grid construction provides a theoretical foundation for the development of LCR, which focuses on the power grid's capacity to resist and mitigate the increase in carbon dioxide.

This resistance capacity can be measured by the increase in carbon emissions caused by extreme disasters that disturb the power grid [15]. Specifically, such disturbances lead to the replacement of low-carbon energy with high-carbon energy, and this increases carbon emissions. One reason for this is that new energy sources are more sensitive to meteorological and environmental factors, making them less resistant to disruption. In such circumstances, the output from these sources is significantly weakened, leading to power deficits. To maintain stability, thermal power units must assume greater responsibility, thereby increasing the risk of carbon emissions.

The mitigation ability can be assessed by evaluating the timespan required for carbon emissions to recover to the power grid's initial operating level after undergoing reduced operation and recovery following a disturbance. The stronger the resistance ability, the lower the increase in carbon emissions, and the shorter the recovery time span, the stronger the mitigation ability. A higher LCR level can be attributed to a smaller increase in carbon emissions after a power grid disaster and a shorter recovery time. Figure 1 depicts the LCR performance of the power grid from the perspectives of resistance and mitigation abilities. Among them, the recovery time of Grid 1 is less than that of Grid 2, the increase in carbon emission of Grid 1 is less than that of Grid 2, and the resilience level of Grid 1 is stronger than that of Grid 2. Based on the analysis, it is evident that Power Grid 1 exhibits better LCR performance than Power Grid 2.

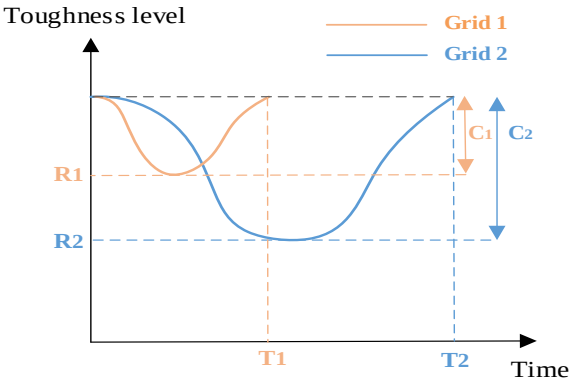

Figure 1. Consider the level of grid LCR for resistance and mitigation.

2.2. LCR Power Grid

The power industry is responsible for the majority of social carbon emissions. With the emergence of a new power system, it is crucial to handle the uncertainties arising from high proportions of renewable energy access and diversified flexible loads. Climate change also needs to be taken into account while assessing the resilience of the power grid. The primary driver of climate change is the increase in carbon emissions. Building an LCR power grid and evaluating its performance from a low-carbon resilience perspective aligns

with the current strategic goals of low-carbon transformation and sustainable development of the power system. Simultaneously, the long-term construction of the power grid during the energy transition under low-carbon policies coupled with the improvement of carbon trading markets will promote the sustained development of LCR power grids towards low-carbonization [2]. Figure 2 illustrates the physical quantities used to evaluate the performance of an LCR power grid concerning different dimensions.

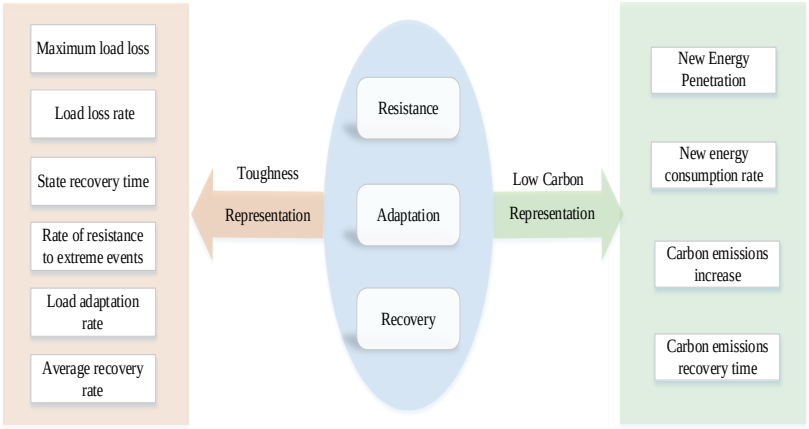

Figure 2. Different dimensions for measuring LCR grid performance.

3. Construction of LCR Index System

The evaluation of LCR power grid performance requires a clear definition of specific disturbance events as different extreme events have different impacts on power grid resilience. This research focuses on power grid resilience, taking into account the impact of frequent ice disasters that have a large impact and long duration. This study only considers transmission line failures, overlooking transmission tower and transformer failures.

The resilience of the power grid when affected by extreme disasters is primarily determined by its ability to respond proactively and recover quickly. The power grid should temporarily reduce its functional level and quickly return to normal operating conditions. The system's operational state curve, usually characterized by the load level, is depicted in Figure 3.

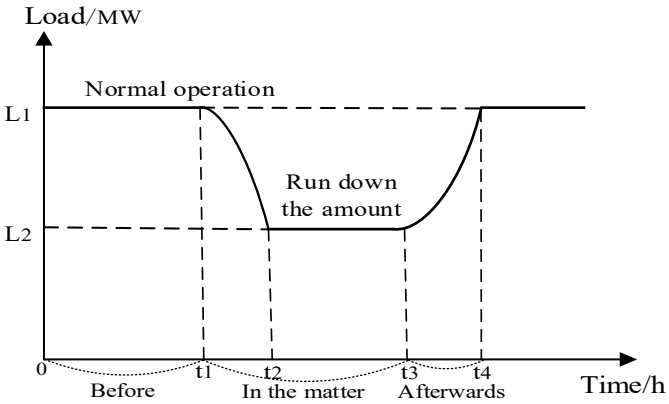

Figure 3. System operating status curve in icy weather.

3.1. LCR Key Indicator System

To assess the impact of ice disasters on the power grid, the entire process is divided into three stages: pre-disaster, during disaster, and post-disaster. Each stage is evaluated using selected indicators within the regional power grid, as shown in Figure 4.

During the pre-disaster stage, the power grid is in its usual operating state, and its low-carbon level is given priority. Extreme disasters may lead to a decrease in new energy

output, resulting in economic losses and increased carbon emissions. However, distributed access to new energy can partially alleviate the resilience pressure [8]. Therefore, different low-carbon levels have distinct comprehensive benefits for the power grid, which can be considered part of its ability to prevent extreme events. During a disaster, the power grid's load loss and resistance capability are evaluated along with its LCR level from the standpoint of resisting an increase in carbon emissions. Following a disaster, particular attention is given to the power grid's recovery capability, including the operational state and its ability to recover carbon emissions to a normal operating level.

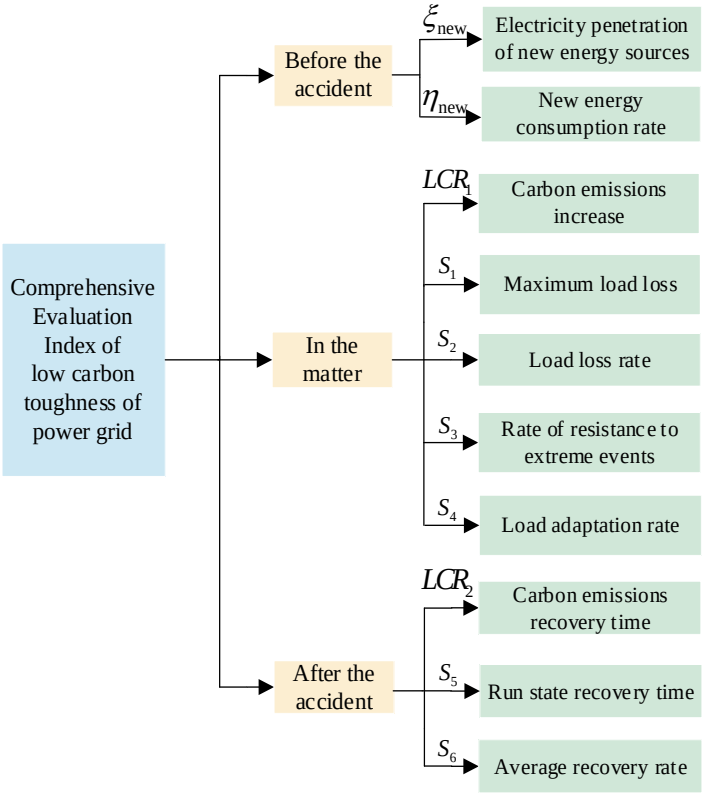

Figure 4. Framework system of comprehensive evaluation indicators for power grids.

The quantitative expressions of the LCR evaluation indicators proposed in this article are as follows:

$$LCR_1 = \lambda_1 \sum_{j=1}^{N} \sum_{t=1}^{T} \left(P_{j,t}^{ENS,1} - P_{j,t}^{ENS,0} \right) - \lambda_2 \sum_{i=1}^{M} \sum_{t=1}^{T} \left(P_{Gi,t}^{0} - P_{Gi,t}^{1} \right) \quad (1)$$

$$LCR_2 = t_4 - t_1 \quad (2)$$

The quantitative expressions of the other indicators are given by Equations (3)–(10). Electricity penetration of new energy sources is established as follows:

$$\xi_{\text{new}} = \frac{\int_0^T \sum_{i=1}^{N_{DG}} P_{Gi}(t)dt}{\int_0^T \sum_{m=1}^{N} P_{Loadm}(t)dt} \quad (3)$$

New energy generation absorption rate is established as follows:

$$\eta_{\text{new}} = \frac{\int_0^T \sum_{i=1}^{N_{DG}} P'_{Gi}(t)dt}{\int_0^T \sum_{i=1}^{N_{DG}} P_{Gi}(t)dt} \quad (4)$$

Maximum load loss represents the maximum interrupt load during the accident [1].

$$S_1 = L_1(t_1) - L_2(t_2) \quad (5)$$

The rate of load loss represents the rate of load interruption during a disaster.

$$S_2 = \frac{L_1(t_1) - L_2(t_2)}{t_2 - t_1} \tag{6}$$

The extreme event resistance rate refers to the power grid's ability to maintain the normal load ratio while resisting the accident.

$$S_3 = \frac{\int_{t_1}^{t_2} L(t)dt}{\int_{t_1}^{t_2} L_1(t)dt} \tag{7}$$

The load adaptation rate indicates the proportion of load capacity that the power grid can maintain from the end of the disaster until it returns to the stable operating state before fault restoration [16,17].

$$S_4 = \frac{\int_{t_2}^{t_3} L(t)dt}{\int_{t_2}^{t_3} L_1(t)dt} \tag{8}$$

The recovery time of the operating state indicates the estimated time required to repair the damaged equipment and restore the system to its normal operation.

$$S_5 = t_4 - t_3 \tag{9}$$

The average recovery rate denotes the average speed of load level recovery in the distribution network when the network is restored to normal through the fault repair and network reconfiguration recovery strategy [14].

$$S_6 = \frac{\int_{t_3}^{t_4} [L(t) - L(t_3)]dt}{t_4 - t_3} \tag{10}$$

Among them, Formulas (3) and (4) are low-carbon (LC) indexes, and Formulas (5)–(10) are resilience (R) indexes.

3.2. LCR Grid Assessment Process

In power network performance evaluation analysis, specific indicators must be identified, and the indicators chosen in this paper depend on the system's operating state curve. Due to the conditions of ice disasters and the continuous repair of transmission lines, the transmission line fault and system operation state change over time, requiring an iterative solution process. The evaluation flowchart is illustrated in Figure 5 with the following specific evaluation steps:

Step 1: Define the LCR evaluation index for the power grid.

Step 2: Utilize meteorological information and power network data to obtain the vulnerability curve of the transmission lines, representing the probability of line failure at each time.

Step 3: Employ the Monte Carlo method to simulate the operational state of each component during extreme weather conditions and generate fault scenarios at different time intervals.

Step 4: The repair time is determined by the system fault set at each time. When the repair time is less than the set step length, the line is considered to be repaired, and the line running state is updated.

Step 5: In the fault scenario, the state curve of the system under an extreme disaster is generated by reducing the load strategy.

Step 6: The LCR index of the power grid is calculated with the state curve diagram, and the appropriate evaluation method is selected to evaluate the LCR performance of the power grid.

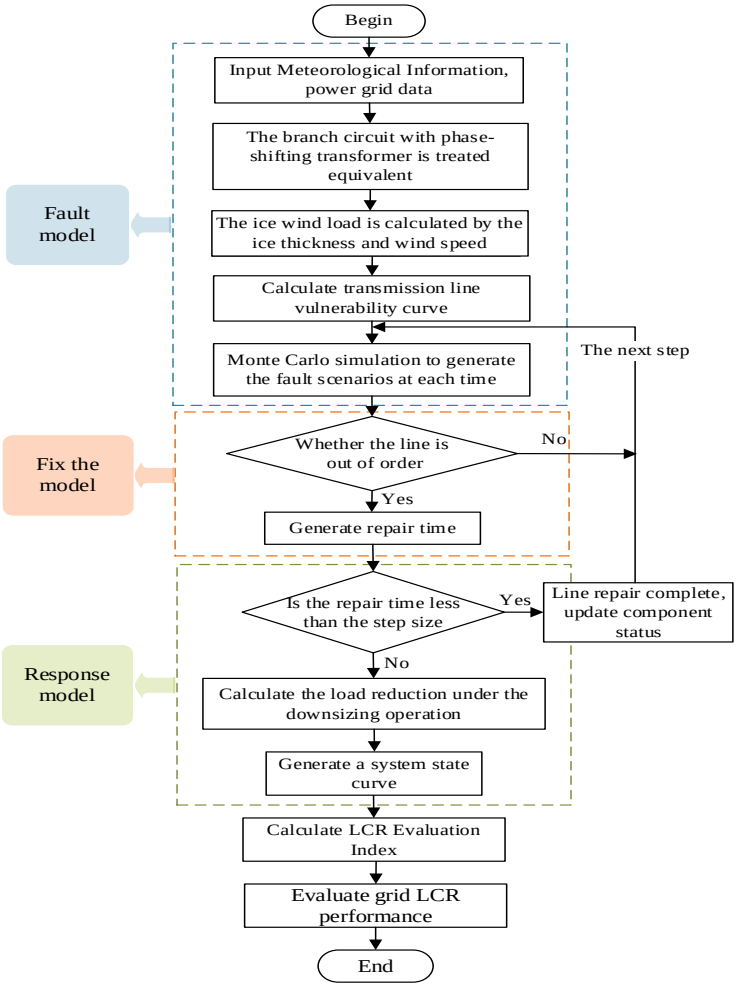

Figure 5. LCR evaluation process for systems in icy weather.

3.2.1. Branch Equivalent Model with Phase-Shifting Transformer

The phase-shifting transformer can be modeled as an ideal transformer with an additional impedance model. To calculate the power flow in a system with a phase-shifting transformer, we need to consider the additional power injection on both sides of the transformer as well as the power injection from the original node during the power flow iteration process. Let us assume that a phase-shifting transformer is installed on the "e" side of the line "e–f". The additional injected power can be represented as follows [11]:

$$\begin{cases} P_{\Delta e} = 2\sin\left(\frac{\varphi}{2}\right)U_e U_f\left[b_{eq}\cos\left(\theta_{ek}+\frac{\varphi}{2}\right)\right] \\ Q_{\Delta e} = 2\sin\left(\frac{\varphi}{2}\right)U_e U_f\left[b_{eq}\sin\left(\theta_{ek}+\frac{\varphi}{2}\right)\right] \\ P_{\Delta f} = -2\sin\left(\frac{\varphi}{2}\right)U_e U_f\left[b_{eq}\cos\left(\theta_{ke}-\frac{\varphi}{2}\right)\right] \\ Q_{\Delta f} = -2\sin\left(\frac{\varphi}{2}\right)U_e U_f\left[b_{eq}\sin\left(\theta_{ke}-\frac{\varphi}{2}\right)\right] \end{cases} \tag{11}$$

3.2.2. Transmission Line Fault Model

The primary cause of line faults during ice disaster weather is the accumulation of excessive ice thickness due to prolonged low-temperature conditions, surpassing the line's capacity to withstand it. In [18], a straightforward model for ice cover thickness is proposed with the following formula:

$$R_{eq} = (T/\pi\rho_I)\sqrt{(\omega\rho_0)^2 + (3.6vW)^2} \tag{12}$$

The ice load is defined to characterize the ice thickness of the line, which is the disaster factor. The ice load per unit length of the line can be expressed as follows [19]:

$$L_I = 9.8 \times 10^{-3} \rho_I \pi R_{eq}(R_{eq} + D) \tag{13}$$

On the basis of icing, the wind load per unit length of a line can be expressed as follows:

$$L_W = 6.964 \times 10^{-3} S {v_g}^2 (2R_{eq} + D) \tag{14}$$

The impact of transmission line tension, gravity resulting from line icing, and horizontal forces induced by strong winds are all taken into account. The magnitude and direction of the wind load caused by ice can be expressed as follows:

$$\begin{array}{c} L_{WI} = \sqrt{L_I^2 + L_W^2} \\ \theta = \arctan \frac{L_W}{L_I} \end{array} \tag{15}$$

Based on the ice wind load, the line failure probability can be obtained as follows:

$$P_f = \begin{cases} 0 & L_{WI} \le a_{WI} \\ \exp\left[\frac{0.6931(L_{WI} - a_{WI})}{b_{WI} - a_{WI}}\right] - 1 & a_{WI} < L_{WI} < b_{WI} \\ 1 & L_{WI} \ge b_{WI} \end{cases} \tag{16}$$

where a_{WI} and b_{WI} are the threshold value; the concrete calculation formula refers to the Ref. [20].

3.2.3. Power System Repair and Response Model

After a transmission line failure, it is crucial to implement appropriate strategies for component repair. The duration required for the operation to recover each line should consider optimistic time t_0, pessimistic time t_p, and most likely time t_m estimates for line restoration. These values are primarily estimated based on the operator's experience and the significance of the faulty line within the regional power network. In Ref. [21], detailed recovery time parameters for IEEE 30-node transmission lines are provided. Ref. [22] suggests that the beta distribution is better suited for simulating repair time. The expected value t_e and the standard deviation σ_t can be expressed as follows:

$$\begin{cases} t_e = \frac{t_0 + 4t_m + t_p}{6} \\ \sigma_t = \frac{t_p - t_0}{6} \end{cases} \tag{17}$$

The occurrence of an ice disaster requires a combination of continuous low temperatures and freezing rain, among other conditions. During the middle and later stages of icing, the most severe consequence can be transmission line outages, leading to the grid being divided into multiple subsystems or even isolated islands. To maintain the stability and secure operation of the entire power grid, load reduction measures need to be implemented. An optimal load-shedding model based on DC power flow is established in this paper [23]. Equation (18) is the objective function to minimize the amount of load shedding; The Formulas (19) and (20) are the system active balance constraint line power flow calculation formula and the DC power flow equation. The Formulas (21)–(23) are the generator active output constraint, load reduction constraint, and line power flow constraint under fault conditions.

$$\min \sum_{d=1}^{N_D} P_{C,d}^f \tag{18}$$

$$P_{L,l}^f = \frac{\theta_d^f - \theta_e^f}{x_l} \tag{19}$$

$$KL^f \sum_{l=1}^{NL} P_{L,l}^f = KG \sum_{j=1}^{N_G} P_{G,j}^f - KD \sum_{d=1}^{N_D} (P_{D,d} - P_{C,d}^f), \forall n \in N \tag{20}$$

$$P_{G,j}^{\min} \le P_{G,j} \le P_{G,j}^{\max}, \forall j \in N_G \tag{21}$$

$$0 \le P_{C,d} \le P_{D,d}, \forall d \in N_D \tag{22}$$

$$-P_{L,\max,l}^{LTE} \le P_{L,l}^f \le P_{L,\max,l}^{LTE}, \forall l \in N_l \tag{23}$$

where KL^f, KG, and KD are the node-branch correlation matrix, node-generator correlation matrix, and node-load correlation matrix under fault state.

4. LCR Index Evaluation Realization

4.1. FAHP–AEWM-Based Weight Setting

4.1.1. Fuzzy Analytic Hierarchy Process

FAHP integrates fuzzy set theory into AHP, effectively addressing the issues of judgment matrix consistency and human thinking variations. By incorporating fuzzy set theory, FAHP allows for a more flexible and nuanced representation of decision-maker preferences, accommodating the inherent uncertainties and imprecisions in human judgment. This integration enhances the reliability and accuracy of the decision-making processes that rely on AHP.

Step 1: Establishing the hierarchical model

To address the evaluation of the low-carbon toughness of the power grid, this paper constructs the following hierarchical structure. As shown in Figure 6.

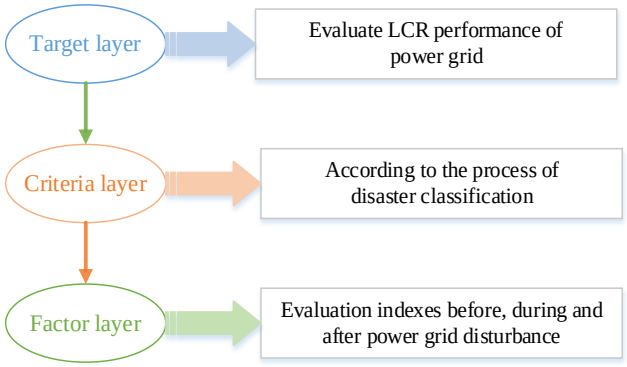

Figure 6. Evaluate the hierarchy of grid LCR performance.

Step 2: Constructing the fuzzy complementary judgment matrix

In the fuzzy AHP, the relative importance of each index at the same level and the subordinate relationship between two factors are evaluated. A matrix is established, denoted as $A = (a_{ij})_{n \times n}$, if the following conditions are met:

$$\begin{cases} a_{ii} = 0.5 & i = 1, 2, \cdots, n \\ a_{ij} + a_{ji} = 1 & i, j = 1, 2, \cdots, n \end{cases} \tag{24}$$

The resulting matrix is referred to as the fuzzy complementary judgment matrix. Additionally, we employ a scale ranging from 0.1 to 0.9 to divide the relative importance between the two indexes. This scale represents the maximum level that individuals can accept from a psychological standpoint. If the scale is further divided into more detailed intervals, it may lead to confusion and hinder accurate judgment [24]. The specific subdivisions of this scale are described in Ref. [25].

Step 3: Weight solution

Based on the established fuzzy complementary judgment matrix, the weight of each index can be calculated using the following formula:

$$w_i = \left(\sum_{j=1}^{n} a_{ij} + \frac{n}{2} - 1 \right) \Big/ n(n-1) \tag{25}$$

The weight vector of the matrix A is as follows:

$$w\prime_i = (w_1, w_2, \cdots, w_n)^T \tag{26}$$

To be satisfied, $w_i \geq 0$, $\sum_{i-1}^{n} w_i = 1 (i = 1, 2, \cdots, n)$.

Then, you can obtain the characteristic matrix A of the judgment matrix as follows:

$$W' = (w_{ij})_{n \times n} \tag{27}$$

To be satisfied, $w_{ij} = w_i / (w_i + w_j) (i, j = 1, 2, \cdots, n)$.

Step 4: Consistency test

To assess the reasonableness of the weight calculation results, it is important to consider that FAHP is a subjective method for determining weights. If the deviation consistency is too significant, it indicates a large deviation in the calculation results of the weight vector. In such cases, the weight vector cannot be reliably used as a basis for decision-making [26]. The consistency principle is typically evaluated using the compatibility principle. The complete consistency of the fuzzy complementary judgment matrix A, along with its characteristic matrix $W\prime$, is equivalent to its own complete consistency [27]. The indicators of compatibility are as follows:

$$I(A, T) = \frac{1}{n^2} \sum_{i=1}^{n} \sum_{j=1}^{n} \left| a_{ij} + w_{ij} - 1 \right| \tag{28}$$

Generally, if the compatibility index $I(A, T) < 0.1$ is met, the consistency test is considered to pass. If not, the values in the matrix are adjusted, and a re-evaluation is conducted until the consistency principle is satisfied.

Step 5: Determining the subjective weight of indicators

Through a layer-by-layer calculation of weights, we can obtain the weight ranking of the factor layer for the target layer. The weight of the criteria layer is denoted as $\dot{W}$.

4.1.2. Anti-Entropy Weight Method

The AEWM is an objective weight determination method that improves upon the entropy weight method. It addresses the weak weight contrast generated with the anti-entropy weight method and complements the advantages of the FAHP method. AEWM possesses the characteristics of stronger index fluctuation, smaller entropy value, and larger weight coefficient.

The calculation steps for AEWM are as follows:

Step 1: Standardization of indicators

Let the problems evaluated have m evaluation objects and n evaluation indexes. The metric value is $x_{ij} (i = 1, 2, \cdots, n; j = 1, 2, \cdots, m)$, and the evaluation matrix is $X = (x_{ij})_{n \times m}$.

Step 2: Determine the anti-entropy value of each index

According to the evaluation matrix, the anti-entropy of each index is as follows [28]:

$$h_i = -\sum_{i=1}^{m} r_{ij} \ln(1 - r_{ij}) \tag{29}$$

Step 3: The objective weight of the index is as follows:

$$w_i'' = h_i \Big/ \sum_{i=1}^{n} h_i \, (i = 1, 2, \ldots, n) \tag{30}$$

That is, based on the FAHP–AEWM method, the comprehensive weight of the index set is denoted as $W = (w_i)_{n\times 1}$. The formula for calculating this weight is as follows:

$$\omega_i = \omega_i' \omega_i'' \Big/ \sum_{i=1}^{n} \omega_i' \omega_i'' \, (i = 1, 2, \ldots, n) \tag{31}$$

4.2. Comprehensive Evaluation of Indicators Based on FCE–COG

After obtaining the evaluation matrix, the fuzzy comprehensive evaluation (FCE) method typically evaluates the index based on the principle of maximum membership degree while disregarding the membership degrees of other evaluation grades [29]. However, to address the limitations of this approach, the evaluation result can be defuzzified using the barycenter method. This helps to compensate for the shortcomings and enhance the accuracy of the evaluation.

Steps of fuzzy comprehensive evaluation [30]:

Step 1: Determine the factor set of the evaluation object $U = \{u_1, u_2, \cdots, u_n\}$
Step 2: Determine the comment set V

The comment set is divided into five grades based on the comprehensive performance of the power grid. The set is represented as $V = \{v1, v2, v3, v4, v5\}$ = {good, better, general, worse, poor}, and each grade is expressed by specific values within a certain range $(0, 1)$, denoted as $V = \{0.9, 0.7, 0.5, 0.3, 0.1\}$.

Step 3: Determine the fuzzy judgment matrix

$$R = \begin{pmatrix} r_1 \\ \cdots \\ r_n \end{pmatrix} = \begin{pmatrix} r_{11} & \cdots & r_{15} \\ \vdots & \ddots & \vdots \\ r_{n1} & \cdots & r_{n5} \end{pmatrix} \tag{32}$$

where r_{ij} is the degree of u_i subordination for v_j. The normal membership function is $\mu_a = e - \left\{ \left[(u_i - v_j)/\sigma \right]^2 \right\}$ selected as the membership function of each evaluation index to the comment set [31], which σ is the standard deviation of the comment set.
Step 4: Calculate the fuzzy comprehensive evaluation set B

$$B = W^T R = \{b_1, b_2, \cdots, b_5\} \tag{33}$$

Taking into account the impact of multiple attribute factors on the actual operation state of the power grid, a multi-level fuzzy comprehensive evaluation method is introduced. The essence of this method lies in obtaining the fuzzy evaluation value for the upper level through the lowest level and ultimately deriving the fuzzy comprehensive evaluation result for the target level. This approach enables a comprehensive assessment that considers the interplay of various attribute factors within the power grid's operational context.

Step 5: Calculate the center of gravity

For $U = \{u_1, u_2, \cdots, u_n\} \subset R$, the membership function $\mu_A(x)$ of a fuzzy set U over a fuzzy set A, the center of gravity can be expressed as:

$$G_A = \sum_{i=1}^{n} x \cdot \mu_A(x) \Big/ \sum_{i=1}^{n} \mu_A(x) \tag{34}$$

After obtaining the final evaluation matrix, the first step is to calculate the center of gravity $G = (g_i)_{1\times n}$ of the fuzzy set for each factor set and establish an evaluation index $a = G\dot{W}$. The comprehensive evaluation result is determined as the evaluation grade that is closest to a. This allows for a more accurate assessment based on the proximity of the evaluation grade to the calculated center of gravity.

5. Example Analysis

Taking the improved IEEE 30-node system as an example, the LCR level of the power network is evaluated using the defined index. In this evaluation, the 8-node thermal power unit is replaced by a wind farm, and a phase-shifting transformer is added between node 5 and node 7. The phase-shifting gears are set to modify the equivalent impedance of the access system. The modified diagram of the IEEE 30-node system is illustrated in Figure 7.

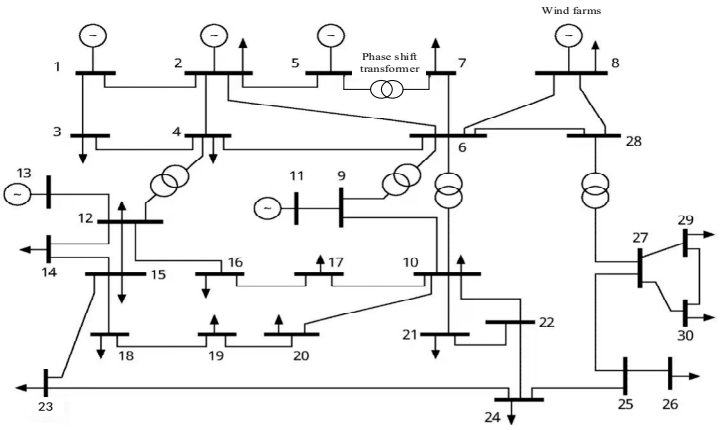

Figure 7. Modified IEEE 30-node system diagram.

Taking into account the conditions of an ice disaster, the maximum anti-ice thickness allowed in the design system is set at 20 mm with a wind speed of 25 m/s. The detailed meteorological information and other parameters related to the ice disaster can be found in Ref. [20].

In this research paper, the duration of the ice disaster is assumed to be 8 days. Considering the need for prolonged low temperatures for transmission line icing, each step length is chosen as 8 h. This results in a division of time into 24 periods, totaling 192 h. By calculating the ice wind load, the fault probability of each transmission line over time is obtained. The failure probability curve for certain lines in the system is depicted in Figure 8. It is observed that the starting time and rate of icing may slightly vary for different lines due to their geographical locations, but the general trend remains consistent.

Since the line fault, repair, and response model proposed in this paper is a linear programming problem, it is solved with CPLEX. The operating state curve of the system can be derived. Figure 9 illustrates two scenarios where the inclusion of phase-shifting transformers is considered. These cases provide visual representations of the system's operating state, showcasing the impact of the phase-shifting transformers in different situations.

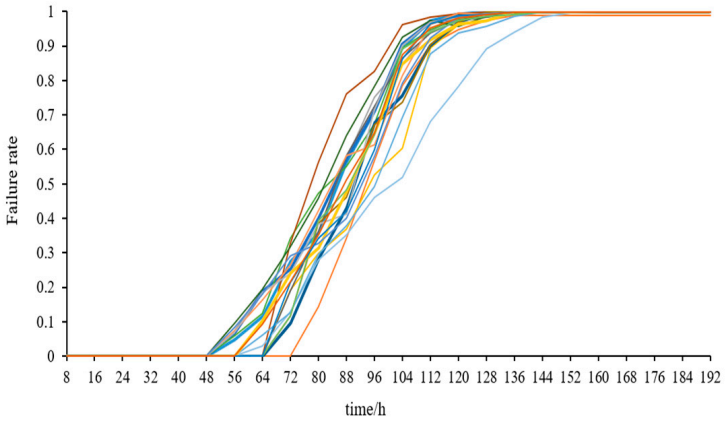

Figure 8. Curve of partial line failure probability over time.

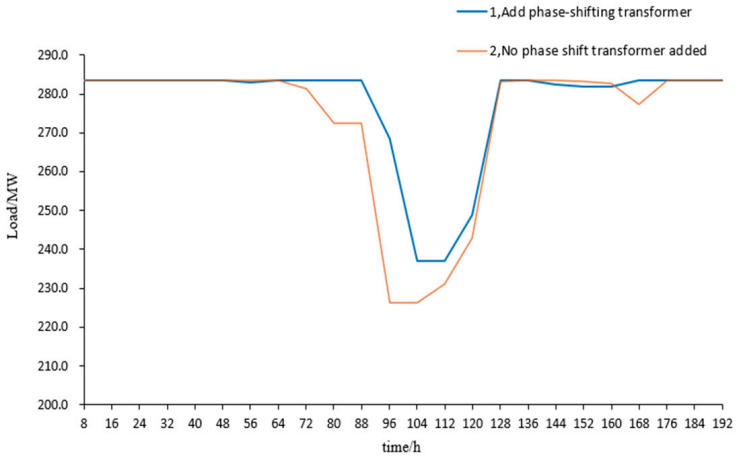

Figure 9. Curve of the operating status of the system under an ice disaster.

Observing the load changes depicted in Figure 9, we can observe that, in Curve 2, the system begins to reduce its load at t = 72 h due to the disturbance caused by the ice disaster. As the ice cover thickness increases, the severity of line breakages worsens, leading to a continuous increase in load loss in order to maintain stable power system operation. At t = 96 h, the power system experiences its maximum load loss, reaching 226.2 MW. At 104 h, the load of the system begins to increase, and at 128 h, the system can resume normal operation. After a certain period of repair, the transmission line gradually returns to its normal operation state.

Curve 1, on the other hand, represents a scenario where the transmission capacity of the system is increased by incorporating phase-shifting transformers onto the original line in the event of a fault. It can be observed that, in this case, the system is able to sustain normal operation for a longer duration after being disrupted. The onset of load reduction occurs later compared to Curve 2, and the system load reaches a maximum loss of 237.1 MW, surpassing Curve 2. Furthermore, the system recovery time has been reduced from 24 h to 16 h. This demonstrates the effectiveness of incorporating phase-shifting transformers in enhancing the resilience and efficiency of the power system during ice disaster situations.

5.1. The Index Value Is Calculated

From the above data and load curve, the index values mentioned in this paper can be calculated with Formulas (1)–(10), as shown in Table 1.

Table 1. The value of the grid evaluation index.

Indicator	No Phase Shift Transformer Added	The Phase-Shifting Transformer	Indicator Type
ξ_{new}	0.529	0.529	LC
η_{new}	0.742	0.891	LC
LCR_1	143.93 MW	90.991 MW	LCR
S_1	50.2 MW	42.3 MW	R
S_2	2.258 MW/h	3.419 MW/h	R
S_3	0.9024	0.9613	R
S_4	0.823	0.8792	R
LCR_2	56 h	40 h	LCR
S_5	24 h	16 h	R
S_6	16.217 MW/h	18.675 MW/h	R

Table 1 provides further evidence supporting the benefits of incorporating a phase shifter into the transmission line. The data reveal that this addition results in a reduction in carbon emissions by 36.78% and a decrease in carbon emission recovery time by 28.57%. Moreover, the system's LCR performance shows improvement with the inclusion of a phase shifter. Additionally, both the maximum load loss and system recovery time are reduced. This indicates enhancements in acceptance rate, resistance rate, and adaptation rate, underscoring the improved low-carbon and resilience performance of the system after integrating a phase shifter.

Based on the aforementioned analysis, it is evident that the addition of a phase shifter enhances the transmission capacity of the line, ultimately leading to an overall superior system performance. To delve deeper into the data, a comprehensive evaluation method proposed in this paper will be employed for further analysis.

5.2. Subjective Weight Assignment

The subjective weight assigned to each index does not rely on specific values, ensuring that the inclusion of the phase shifter will not alter the outcome. Once the subjective weight vector is obtained using Formulas (24)–(26), it is essential to verify if the consistency requirement is met. This is accomplished by calculating Formula (28) for $I_1 = 0.0375$, $I_2 = 0.0710$, and $I_3 = 0.0360$ and assessing the overall consistency. The result of the subjective weight assignment is $W' = (0.4500, 0.5500, 0.2050, 0.2150, 0.1950, 0.1750, 0.3330, 0.3000, 0.3667)^T$.

5.3. Objective Weight Assignment

Given that the selected indexes are employed to assess the power grid's performance from various perspectives, it is necessary to standardize the index values. These indexes can be categorized into two types, benefit type and cost type, each requiring a specific standardization method as referenced in [32]. Subsequently, the objective weight vector can be computed using Formulas (29) and (30). Finally, the comprehensive weight results for each index can be obtained through FAHP–AEWM, as depicted in Figure 10.

5.4. Comprehensive Evaluation

The fuzzy evaluation matrix for each index can be generated using the membership function. Subsequently, the evaluation matrix for the criterion layer can be obtained by calculating the fuzzy evaluation value, as illustrated in Table 2. To facilitate reference, Case 1 denotes the scenario where the phase-shifting transformer is not added, while Case 2 represents the scenario where the phase-shifting transformer is added.

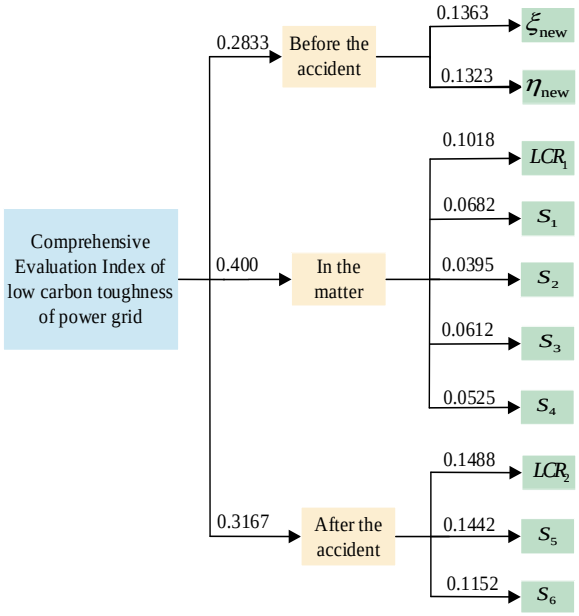

Figure 10. Comprehensive empowerment of power grid evaluation indicators.

Table 2. Benchmark layer evaluation matrix.

Case	Criteria Layer	Evaluation Matrix
case 1	$B_{LCR,1}$	0.0466, 0.1672, 0.2714, 0.1997, 0.0666 0.0412, 0.1673, 0.3136, 0.2717, 0.1089 0.0411, 0.1825, 0.3687, 0.3381, 0.1406
case 2	$B_{LCR,2}$	0.0666, 0.1997, 0.2714, 0.1672, 0.0466 0.1089, 0.2717, 0.3136, 0.1673, 0.0412 0.1406, 0.3381, 0.3687, 0.1825, 0.0411

Upon comparing the aforementioned data, it becomes evident that, after adding the phase-shifting transformer, the ranking of the criterion layer indexes corresponding to each comment set is as follows: general > better > worse > good > poor. Similarly, the ranking of membership degrees is as follows: general > worse > better > poor > good. It can be observed that all indexes attain the highest grade of 'General', and this highest grade remains consistent across both cases. The main discrepancy lies in the second-grade rating. To obtain a precise evaluation value for power network performance, the center of gravity method is employed to accurately handle the fuzzy results, as presented in Table 3.

Table 3. LCR grid evaluation results.

Case	The Barycenter Vector of the Fuzzy Set in the Criterion Layer	Final Evaluation Indicators and Evaluation Results
case 1	0.4207, 0.4069, 0.4038	$a_{LCR,1} = 0.4098$ (general)
case 2	0.5793, 0.5931, 0.5962	$a_{LCR,2} = 0.5902$ (general)

5.5. Results Analysis

From the weight distribution of Figure 10, the weight (0.4) is the largest in macro-scale, and (0.3167) is the second in post-accident. The weight distribution shows that, when the extreme event occurs, the resistance of the power grid LCR is most affected by the strength of the comprehensive evaluation results, especially in the system. In addition to considering the loss of load resistance, the ability to adapt and recover after the event is also a significant part of the assessment because the time it takes for the system to regain stability depends on how quickly it recovers; in addition, the ability to prevent in advance

also cannot be ignored. On the one hand, the better the prevention measures, the less the loss of power grid operation in extreme disasters; on the other hand, the access to renewable energy for the system response to disasters has certain advantages.

The evaluation matrix represents the close degree of each index to the comment set, which is essentially decided by the weight and the index value. It can be observed in Table 2 that the result of prior layer membership ranking is better than that before adding the phase-shifting transformer. The reason is that, in terms of the weight distribution, there is not much difference between the two indexes in advance. The main difference is the index value. Obviously, after adding the phase-shifting transformer, the new energy absorption rate is higher, so we engage in the front-level evaluation; the evaluation grade of the power grid is higher after joining. The increase in new energy efficiency will also bring low-carbon benefits, reducing carbon emissions to a certain extent and shortening the recovery time of carbon emissions. At the same time, the addition of phase shifters has a positive impact on the grid in both the resilience and recovery stages; therefore, both in-event and post-event levels are closer to the higher ratings of comment sets.

The final Table 3 evaluation results are in line with the previous discussion. For the two cases with or without the phase-shifting transformer, the performance of the power grid is average, but the LCR evaluation value of the power grid is 0.5902 after adding the phase-shifting transformer, which is higher than that before adding the phase-shifting transformer; this shows that the evaluation method used in this paper can make a correct evaluation of LCR performance of a power grid. The evaluation results also show that the LCR performance of a power grid can be improved by adding a phase-shifting transformer.

6. Conclusions

In this paper, a novel LCR assessment index is proposed based on existing resilience assessments, focusing on carbon emission resistance and mitigation capacity. An assessment framework is constructed, encompassing the entire process of ice disasters. After establishing the evaluation index system for power grids in response to ice disasters, the LCR performance of the power grid in tackling such extreme events is evaluated using comprehensive weighting, fuzzy evaluation, and precise treatment methods. The validity of the proposed index and methodology is confirmed through comparative analysis. The conclusions were as follows:

(1) With the phase-shift transformer, the power grid shows superior performance before, during, and after the extreme disaster. The absorption of new energy before the event to reduce the maximum load loss, the increase in the rate of resistance and adaptation, and after the increase in resilience are reflected.

(2) With the penetration of the low-carbon concept, the low-carbon resilience index based on the increase in carbon emissions and the recovery time of carbon emissions proposed in this paper can better evaluate the comprehensive performance of a power grid under extreme disasters. At the same time, low carbon and resilience are more mutually reinforcing. The more new energy access, the better the low-carbon benefits of the power grid, while flexible resources on the power grid to resist the occurrence of disasters will also have a positive impact.

Additional research can further analyze the influence of the installation location of the phase-shift transformer and the energy storage resource on the low-carbon toughness of a power grid. In the future, multi-energy deep coupling is both an opportunity and a challenge. Based on the research in this paper, we can continue to expand the LCR grid evaluation index system and add the consideration of low-carbon factor while exploring more means of improving resilience, and the LCR performance of a power grid is evaluated more comprehensively.

Author Contributions: Conceptualization, J.Z.; Methodology, H.C.; Writing—original draft, B.Z.; Writing—review & editing, J.Z., P.Y., B.Z., S.Z. and Z.L.; Project administration, J.Z., H.C., P.Y. and Z.L.; Funding acquisition, Z.L. All authors have read and agreed to the published version of the manuscript.

Funding: This research was funded by Technology project of State Grid Hebei Electric Power Co., Ltd. (No. kj2022-016).

Data Availability Statement: The datasets supporting the conclusions of this article are included within the article.

Conflicts of Interest: The authors declare no conflict of interest.

Nomenclature

Indices and Sets	
e, f	Index for buses
m	Index for scenarios
a_{ij}	Index for the relative importance of each index at the same level
r_{ij}	Index for degree of u_i subordination for v_j
N_D, N_G, N_l, N	Set for loads, generators, lines, nodes
Parameters	
N_{DG}	Number of new energy power plants
N	Number of buses
M	Number of new energy source buses
T	Duration of the ice disaster
LCR_1	Increase in carbon emissions of the power grid
LCR_2	Time for carbon emissions of the power grid to recover
λ_1	Carbon emission coefficients of the power plant
λ_2	New energy emission reduction coefficient
ξ_{new}	Electricity penetration of new energy sources
η_{new}	New energy generation absorption rate
R_{eq}	Thickness of ice cover (mm)
L_I	Ice load (N/m)
L_W	Wind load (N/m)
S	Pitch factor
v_g	Wind speed (m/s)
t_e	The expected value
σ_t	The standard deviation
$W\prime$	The characteristic matrix of the judgment matrix
a	Evaluation index
Constants	
L_1	The amount of load under normal system operating conditions
L_2	The amount of load under system derating operation
a_{WI}, b_{WI}	Threshold value
ρ_I	Density of ice, 0.9 g/cm^3
ρ_0	Density of water, 1.0 g/cm^3
D	Wire diameter
t_0	Optimistic time for line recovery
t_p	Pessimistic time for line recovery
t_m	Most likely time for line recovery
$P_{D,d}$	The active load of load d
$P_{G,j}^{\min}$, $P_{G,j}^{\max}$	The minimum and maximum output of a generator
$P_{L,\max,l}^{LTE}$	Long-term emergency limit of Line Power flow under fault condition
Variables	
t_1	System operating time: moment of the disaster occurrence
t_2	Moment the power grid enters a stable operation at reduced capacity
t_3	The moment when the ice disaster dissipates
t_4	The moment when the power grid resumes normal operation
$P_{j,t}^{ENS,0}$	Load shedding amount of the system in normal operating conditions
$P_{j,t}^{ENS,1}$	Load shedding amount of the system in a fault state
$P_{Gi,t}^{1}$	New energy grid-connected power in fault operating conditions
$P_{Gi,t}^{0}$	New energy grid-connected power in normal operating conditions

$P_{Gi}(t)$	Power of new energy units i for time period t
$P_{Loadm}(t)$	Power of load m for time period t
$P_{Gi}{}'(t)$	Power of new energy units i or time period t
$L(t)$	Load at time period t
$P_{\Delta e}$, $P_{\Delta f}$	Additional active power injected into the bus
$Q_{\Delta e}$, $Q_{\Delta f}$	Additional reactive power injected into the bus
U_e, U_f	Voltage amplitudes of the bus
φ	No-load phase-shifting angle of the phase-shifting transformer
b_{eq}	Equivalent admittance of the phase-shifting transformer
θ_{ek}	Bus phase difference of the two sides of the phase-shifting transformer
ω	The precipitation per hour (mm/h)
v	Wind speed at the location (m/s)
W	Content of liquid water in the air, $W = 0.067\omega^{0.846}$
$P^f_{C,d}$	Load d the amount of load cut off in the failure state
$P^f_{G,j}$	Active power output of generator j under fault condition
$P^f_{L,l}$	Power flow of Line l in a fault state
θ^f_d, θ^f_e	The voltage phase angle of the beginning node d and the end node e of line l under fault condition
x_l	The DC resistance of line l

References

1. Chen, L.; Deng, X.Y.; Chen, H.K.; Shi, J. Power System Resilience Assessment and improvement. *Power Syst. Prot. Control.* **2022**, *50*, 11–22.
2. Ruan, Q.T.; Xie, W.; Xu, Y.; Hua, B.; Song, P.; He, J.H.; Zhang, Q.Q. Concept and key features of flexible power grid. *Chin. J. Electr. Eng.* **2020**, *40*, 6773–6784.
3. Fotopoulou, M.; Rakopoulos, D.; Petridis, S. Decision Support System for Emergencies in Microgrids. *Sensors* **2022**, *22*, 9457. [CrossRef] [PubMed]
4. Wu, Y.K.; Chen, Y.C.; Chang, H.L.; Hong, J.S. The Effect of Decision Analysis on Power System Resilience and Economic Value During a Severe Weather Event. *IEEE Trans. Ind. Appl.* **2022**, *58*, 1685–1695. [CrossRef]
5. Li, Z.K.; Wang, F.S.; Gu, W.Y.; Mi, Y.; Ji, L. Elasticity assessment of smart distribution networks in extreme weather. *Power Syst. Autom.* **2020**, *44*, 60–68.
6. Wang, Y.; Huang, T.; Li, X.; Tang, J.; Wu, Z.; Mo, Y.; Xue, L.; Zhou, Y.; Niu, T.; Sun, S. A Resilience Assessment Framework for Distribution Systems Under Typhoon Disasters. *IEEE Access* **2021**, *9*, 155224–155233. [CrossRef]
7. Chen, Y.; Yang, Y.; Liu, Y.; Lu, Q.; Yang, M.; Zhang, R.; Liu, J. An Optimization Strategy for Power System Partition Recovery Considering Grid Reconfiguration Efficiency and Path Reliability. In Proceedings of the 2023 6th International Conference on Energy, Electrical and Power Engineering (CEEPE), Guangzhou, China, 12–14 May 2023; pp. 1449–1454.
8. Ruan, Q.T.; Mei, S.W.; Huang, X.D.; Chen, Y. Challenges and prospects for improving the resilience of low-carbon urban power grids. *Chin. J. Electr. Eng.* **2022**, *42*, 2819–2830.
9. Kang, C.Q.; Yao, L.Z. Key scientific problems and theoretical research framework of high-proportion renewable energy power system. *Power Syst. Autom.* **2017**, *41*, 1–11.
10. Milano, F.; Dörfler, F.; Hug, G.; Hill, D.J.; Verbič, G. Foundations and challenges of low-inertia Systems (Invited Paper). In Proceedings of the 2018 Power Systems Computation conference-(PSCC), Dublin, Ireland, 11–15 June 2018.
11. Shen, T. *Application of Phase-Shifting Transformer in Power System*; North China Electric Power University: Beijing, China, 2018.
12. Qu, Z.Y.; Liao, H.X.; Yu, J.L.; Gao, H.; Su, A.L.; Ge, W.C.; Liu, C. Study on phase-shift transformer location problem to eliminate line overload. *Grid Technol.* **2002**, *25*, 30–32+44.
13. Yu, J.L.; Liu, C. Power flow control based on unified characteristics of phase shifters. *Chin. J. Electr. Eng.* **1994**, *14*, 1–5+10.
14. Cui, X.; Zhao, K.; Zhou, Z.; Huang, P. Examining the uncertainty of carbon emission changes: A systematic approach based on peak simulation and Resilience Assessment. *Environ. Impact Assess. Rev.* **2021**, *91*, 106667. [CrossRef]
15. Zhang, J.M.; Wang, Y.K.; Xue, Y.S.; Xue, F.; Chang, K. Natural disaster chain-power system-Bayesian network estimation of carbon emission change. *Power Syst. Autom.* **2023**, *47*, 1–11.
16. Wu, J.; LÜ, L.; Huang, Y.; Li, X.C.; Ji, C.L. Evaluation method and lifting strategy of distribution network elasticity in whole disaster process. *J. Power Syst. Their Autom.* **2021**, *33*, 32–42.
17. Xiao, Z.W.; Wang, G.Q.; Zhu, J.M.; Chen, H.J. Evaluation and construction method of power grid resilience capacity for emergencies. *Syst. Eng.-Theory Pract.* **2019**, *39*, 2637–2645.
18. Jones, K.F. A simple model for freezing rain ice loads. *Atmos. Res.* **1998**, *46*, 87–97. [CrossRef]
19. Zhao, N.Y. *Resilience Assessment of Transmission System under Ice Disaster and Strategy of Full-Time Resilience Enhancement*; Tianjin University: Tianjin, China, 2020.

20. Feng, W.M. *Grid Operation Risk Assessment and Network Protection Considering Ice Disaster*; Harbin Institute of Technology: Harbin, China, 2014.
21. Huang, W.X.; Wu, J.; Guo, Z.H.; Chen, Y.H.; Liu, Z.C. Power Grid Resilience Assessment and differential planning under typhoon disaster. *Power Syst. Autom.* **2023**, *47*, 84–91.
22. Mota, A.A.; Mota, L.T.M.; Morelato, A. Visualization of Power System Restoration Plans Using CPM/PERT Graphs. *IEEE Trans. Power Syst.* **2007**, 1322–1329. [CrossRef]
23. Tang, W.H.; Yang, Y.H.; Li, Y.J.; Lu, J.Z.; Wu, Q.H. Research on transmission system elasticity evaluation and lifting measures under extreme meteorological disasters. *Chin. J. Electr. Eng.* **2020**, *40*, 2244–2254+2403.
24. Li, J.Q. *Research on Risk Evaluation of Intellectual Property Pledge Financing Based on Fuzzy Analytic Hierarchy Method*; University of Electronic Science and Technology of China: Chengdu, China, 2021.
25. Gong, G.B. *Diagnosis of Regional Power Grid Development Based on Fuzzy Analytic Hierarchy Process*; China University of Mining and Technology: Beijing, China, 2019.
26. Liu, Q. *Application Research on Risk Management of Small-Scale Power Grid Infrastructure Based on Fuzzy Analytic Hierarchy Process*; Tianjin University: Tianjin, China, 2018.
27. Yang, Y.H.; LÜ, Y.J. Consistency test of fuzzy judgment matrix. *Stat. Decis. Mak.* **2018**, *34*, 78–80.
28. Zhang, H.R.; Han, D.; Liu, Y.J.; Song, Y.Q.; Yan, Z.; Sun, Q.; Zhang, Y.B. Evaluation of smart grid based on anti-entropy weight method. *Power Syst. Prot. Control.* **2012**, *40*, 24–29.
29. LÜ, P.P.; Zhao, J.Q.; Li, D.C.; Zhu, Z.F. Evaluation index system and comprehensive evaluation method. *Grid Technol.* **2015**, *39*, 2245–2252.
30. Zhang, Y. *Application Research Based on Fuzzy Analytic Hierarchy-Fuzzy Comprehensive Evaluation Model*; Anqing Normal University: Anqing, China, 2022.
31. Zeng, Y.; Jia, H.P.; Yang, J.; Wang, W.; Zhong, Y.; Han, J.S.; Liu, D.N. Evaluation method of synthetic contribution degree of virtual power plant based on fuzzy analytic hierarchy process-entropy weight method-approximate ideal solution ordering method. *Mod. Electr.* **2023**, 1–8. [CrossRef]
32. Lin, J.K.; Li, T.F.; Zhao, Z.M.; Zheng, W.H.; Liu, T. Black-start scheme evaluation of power system based on entropy weight fuzzy comprehensive evaluation model. *Grid Technol.* **2012**, *36*, 115–120.